Ashok Kumar[1], Shilpa Sood[1], Pankaj Thakur[2], Naresh Kumar[2]

SAFETY ANALYSIS IN AN ISOTROPIC MATERIAL DISC FITTED WITH A RIGID SHAFT SUBJECTED TO THERMO-MECHANICAL LOAD BY USING TRANSITION THEORY

ANALIZA SIGURNOSTI DISKA OD IZOTROPNOG MATERIJALA SA KRUTIM VRATILOM OPTEREĆEN TERMOMEHANIČKI PRIMENOM TEORIJE PRELAZNIH NAPONA

Originalni naučni rad / Original scientific paper
UDK /UDC:

Rad primljen / Paper received: 2.06.2021

Adresa autora / Author's address:
[1)] Department of Mathematics, Career Point University Hamirpur, Himachal Pradesh, India
[2)] Depart. of Mathematics, Faculty of Science and Technol., ICFAI University Baddi, Solan, India
email: pankaj_thakur15@yahoo.co.in

Keywords
- thermo-mechanical load
- stresses
- displacement
- rubber and copper disc

Ključne reči
- termomehaničko opterećenje
- naponi
- pomeranja
- gumeni i bakarni disk

Abstract

The objective of the paper is to present safety analysis in an isotropic material disc fitted with a rigid shaft under the influence of thermo-mechanical load by using Seth's transition theory. The rubber material disc must require higher angular speed to yield at the internal surface as compared to the copper material disc. Performance of the mechanical load places the copper disc on the safer side of the design as compared to rubber disc with temperature, because the radial stress is less for the rotating disc without temperature as compared to the disc with temperature, which leads to the idea of stress saving and minimizing the possibility of fracture of the isotropic rotating disc. Results are discussed numerically and depicted graphically.

Izvod

Predstavljena je analiza sigurnosti za disk od anizotropnog materijala sa krutim vratilom, pod dejstvom termomehaničkog opterećenja, primenom teorije prelaznih napona Seta. Disk od gume zahteva veću ugaonu brzinu za pojavu tečenja na unutrašnjoj površini, u poređenju sa diskom od bakra. Ponašanje pod dejstvom mehaničkog opterećenja pokazuje da je bakarni disk bezbedniji sa aspekta projektovanja u odnosu na gumeni disk sa uticajem temperature, jer je radijalni napon manji pri rotaciji diska bez dejstva temperature, u poređenju sa uticajem temperature na disk, čime se nagoveštava ideja smanjenja napona i mogućnosti pojave loma izotropnog rotirajućeg diska. Data je diskusija numeričkih rezultata, koji su predstavljeni i grafički.

INTRODUCTION

The rotating disc of isotropic materials is widely used in fields of mechanics, aerospace, and marine industry for machines and machine elements like the rotors of rotating flywheels, high speed gear engines, gas turbines, structural engineering, compressors, computer disc drives, chemical processing and aerospace industries etc. Güven et al. /4/ have investigated the problem of solid disc with external pressure and non-uniform heat source by Tresca's yield condition and plane stress. Eraslan et al. /5/ investigated the thermo elastic-plastic deformation of a rotating disk by using Tresca and von Mises criteria. Alexandrova et al. /6/ have investigated the problem of stress distribution in a plastically anisotropic disk. The thermo elastic-plastic stress distribution in a composite disc subjected to thermal condition has been analysed by Sayman et al. /7/. Faruk et al. /8/ calculated residual stress components by using elastic and elasto-plastic solution results. He also showed the positions of improved thermal and residual stresses. Altan et al. /9/ examined the problem of thermal stress in an orthotropic aluminium composite disc subjected to parabolic thermal load distribution. Bhowmick et al. /10/ have obtained the solution of angular speed for external loaded rotating solid disc by variational method. Sen et al. /11/ obtained the thermal stresses in a thermoplastic composite disc - directionally reinforced with steel fibres by using finite elements. Bayat et al. /12/ have investigated thermal stresses in a functionally graded rotating disc having variable thickness and load. Bhowmick et al. /13/ discussed study of external loaded rotating discs under shrink fit. Damircheli et al. /14/ obtained the solution of rotating FG-discs of variable thickness and temperature by using finite element method. Kurşun et al. /15/ presented the problem of stresses of functionally graded disc subjected to temperature and mechanical loads. Hassani et al. /16/ investigated the thermal stress distribution in rotating disc with non-uniform thickness by using Runge-Kutta's and finite element (FE) methods. Kurşun et al. /17/ investigate elastic stresses of a hollow disc of functionally graded materials with variable thickness and mechanical load. Thawait et al. /31/ investigate the stress distribution in FGM rotating disc having variable thickness by using exponential, power law, and Mori-Tanaka scheme. Sethi et al. /32/ obtained the solution of isotropic material disc fitted with shaft having mechanical load and density by using transition theory. Mohamed et al. /33/ analysed the optimization of functionally graded rotating disc subjected to thermal condition by using the finite element method. Thakur et al. /18-30, 33-45/ have obtained the solution of the rotating disc made of

orthotropic/transversely isotropic/isotropic materials having density parameter, thermal condition and with rigid shaft/ free boundary condition, by using Seth's transition theory and generalized strain measures.

MATHEMATICAL MODEL

We consider a thermal annular axi-symmetrical isotropic material disc, with internal radius r_i, and external radius r_0, fixed with rigid shaft and rotating with angular velocity ω. Let the disc be of a rubber/copper material with variable density, and the thickness is assumed to be constant with plane stress condition. The density of disc is to be assumed along the radius as:

$$\rho = \rho_0 (r / r_0)^{-m} . \tag{1}$$

Here, we assume that temperature Θ_0 is to be applied on the internal surface of the disc. Let a mechanical load l_0 be applied to the external surface of the disc, as shown in Fig. 1, and the boundary conditions are given:

$$r = r_i, \quad u = 0 \quad \text{and} \quad r = r_0, \quad \tau_{rr} = l_0 . \tag{2}$$

Basic governing equations

Displacement components: displacement components are:

$$u = r(1-\eta), \; v = 0, \; w = dz, \tag{3}$$

where: η is a function of r.

Generalized strain components: generalized strain components are given by Seth /2/:

$$\varepsilon_{rr} \equiv \frac{\partial u}{\partial r} - \frac{1}{2}\left(\frac{\partial u}{\partial r}\right)^2 = \frac{1}{2}\left[1-(r\eta'+\eta)^2\right],$$

$$\varepsilon_{\theta\theta} \equiv \frac{u}{r} - \frac{u^2}{2r^2} = \frac{1}{2}\left[1-\eta^2\right],$$

$$\varepsilon_{zz} \equiv \frac{\partial w}{\partial z} - \frac{1}{2}\left(\frac{\partial w}{\partial z}\right)^2 = \frac{1}{2}\left[1-(1-d)^2\right],$$

$$\varepsilon_{r\theta} = \varepsilon_{\theta z} = \varepsilon_{zr} = 0 , \tag{4}$$

where: $\eta' = d\eta/dr$.

Stress-strain relations: constitutive equations for isotropic material are given by /1, 3/:

$$\tau_{ij} = \lambda \delta_{ij} e_{kk} + 2\mu\varepsilon_{ij} - \xi\Theta\delta_{ij}, \quad (i, j = 1,2,3), \tag{5}$$

where: $\xi = \alpha(3\lambda + 2\mu)$.

Eq. (5) can be written as:

$$\tau_{rr} = \frac{2\lambda\mu}{\lambda+2\mu}[\varepsilon_{rr} + \varepsilon_{\theta\theta}] + 2\mu\varepsilon_{rr} - \frac{2\mu\xi\Theta}{(\lambda+2\mu)},$$

$$\tau_{\theta\theta} = \frac{2\lambda\mu}{\lambda+2\mu}[\varepsilon_{rr} + \varepsilon_{\theta\theta}] + 2\mu\varepsilon_{\theta\theta} - \frac{2\mu\xi\Theta}{(\lambda+2\mu)},$$

$$\tau_{r\theta} = \tau_{\theta z} = \tau_{zr} = \tau_{zz} = 0 . \tag{6}$$

Temperature condition: Θ has to satisfy the Laplace equation as given /3/:

$$\nabla^2\Theta = 0 , \tag{7}$$

$$\frac{d^2\Theta}{dr^2} + \frac{1}{r}\frac{d}{dr}\left(\frac{d\Theta}{dr}\right) \equiv \frac{1}{r}\frac{d}{dr}\left(r\frac{d\Theta}{dr}\right) = 0 ,$$

or

$$\frac{d\Theta}{dr} = \frac{A}{r} ;$$

and have a general solution:

$$\Theta = A(\ln r + A_1) . \tag{8}$$

The temperature satisfying Eq.(7) with the boundary condition:

$$\Theta = \Theta_0 \quad \text{at} \quad r = r_i , \quad \text{and} \quad \Theta = 0 \quad \text{at} \quad r = r_0 , \tag{9}$$

where: Θ_0 is constant; given $A = \Theta_0/\ln(r_i/r_0)$ and $A_1 = -\ln(r_0)$. Substituting the constant values of A and A_1 from Eq.(8), we get: $\Theta = \dfrac{\Theta_0 \ln(r/r_0)}{\ln(r_i/r_0)}$.

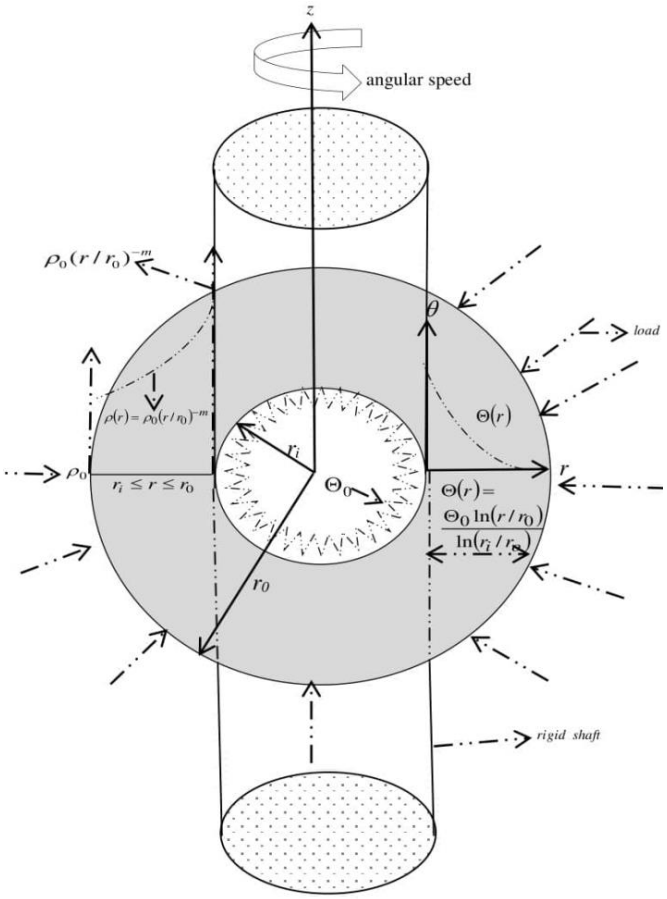

Figure 1. Disc profile.

Strain components: components of strain in terms of stresses are obtained by /1/ and using Eq.(4) we get

$$\varepsilon_{rr} = \frac{\partial u}{\partial r} - \frac{1}{2}\left(\frac{\partial u}{\partial r}\right)^2 = \frac{1}{2}\left[1-(r\eta'+\eta)^2\right] = \frac{1}{E}\left[\tau_{rr} - \left(\frac{1-c}{2-c}\right)\tau_{\theta\theta}\right] + \alpha\Theta ,$$

$$\varepsilon_{\theta\theta} = \frac{u}{r} - \frac{u^2}{2r^2} = \frac{1}{2}\left[1-\eta^2\right] = \frac{1}{E}\left[\tau_{\theta\theta} - \left(\frac{1-c}{2-c}\right)\tau_{rr}\right] + \alpha\Theta ,$$

$$\varepsilon_{zz} = \frac{\partial w}{\partial z} - \frac{1}{2}\left(\frac{\partial w}{\partial z}\right)^2 = \frac{1}{2}\left[1-(1-d)^2\right] = -\frac{(1-c)}{E(2-c)}[\tau_{rr} - \tau_{\theta\theta}] + \alpha\Theta ,$$

$$\varepsilon_{r\theta} = \varepsilon_{\theta z} = \varepsilon_{zr} = 0 , \tag{10}$$

where: $E = \mu(3\lambda + 2\mu)/(\lambda + \mu) = 2\mu(3 - 2c)/(2 - c)$; $c = 2\mu/(\lambda + 2\mu)$; $\nu = (1 - c)/(2 - c)$ in terms of Lame's constant and compressibility factor. Using Eq.(4) into Eq.(6), we get stress components:

$$\tau_{rr}=\frac{2\mu}{n}\left[3-2c-\eta^n\left\{1-c+(2-c)(T+1)^n+\frac{nc\xi\Theta}{2\mu\eta^n}\right\}\right],$$

$$\tau_{\theta\theta}=\frac{2\mu}{n}\left[3-2c-\eta^n\left\{2-c+(1-c)(T+1)^n+\frac{nc\xi\Theta}{2\mu\eta^n}\right\}\right],$$

$$\tau_{r\theta}=\tau_{\theta z}=\tau_{zr}=\tau_{zz}=0\,. \quad (11)$$

Equilibrium equation: the equilibrium equation of the axially symmetric disc in the absence of body force is given as:

$$\frac{d}{dr}(r\tau_{rr})-\tau_{\theta\theta}+\rho\omega^2r^2=0\,. \quad (12)$$

Asymptotic solution at transition points: substituting Eq. (11) into Eq.(12) and using Eq.(9), we obtained the following equation:

$$(2-c)n\eta^{n+1}T(T+1)^{n-1}\frac{dT}{d\eta}=\left[\frac{n\rho\omega^2r^2}{2\mu}+\eta^n\left[1-(T+1)^n-\right.\right.$$

$$\left.\left.-nT\{1-c+(2-c)(T+1)^n\}\right]-\frac{nc\xi\overline{\Theta_0}}{2\mu}\right], \quad (13)$$

where: $\overline{\Theta_0}=\Theta_0/\ln(r_i/r_0)$; $r\eta'=\eta T$; $\eta'=d\eta/dr$ for $T=T(\eta)$ and $\eta=\eta(r)$.

SOLUTION OF THE PROBLEM

An elastic stage can go to plastic stage under internal/ external loading through the transition state /2, 18-30, 33-45/ at transition point $T\to\pm\infty$. We define transition function ψ as:

$$\psi=\frac{n}{2\mu}[\tau_{\theta\theta}-c\xi\Theta]=\left[(3-2c)-\eta^n\{2-c+(1-c)(T+1)^n\}\right]. \quad (14)$$

By taking the logarithmic differentiation we get

$$\frac{d(\log\psi)}{dr}=-\left(\frac{n\eta^nT}{r}\right)\frac{2-c+(1-c)(T+1)^{n-1}\left\{(T+1)+\eta\frac{dT}{d\eta}\right\}}{(3-2c)-\eta^n\{2-c+(1-c)(T+1)^n\}}\,. \quad (15)$$

Using Eq.(13) into Eq.(15) and taking $T\to\pm\infty$ and after integrating, we obtained as:

$$\psi=A_2r^{\nu-1}. \quad (16)$$

From Eq.(14) and Eq.(16), we get:

$$\tau_{\theta\theta}=\left(\frac{2\mu}{n}\right)A_2r^{\nu-1}+\frac{c\xi\Theta_0\ln(r/r_0)}{\ln(r_i/r_0)}\,. \quad (17)$$

Using Eq.(17) into Eq.(12) then after using Eq.(1), and integrating, we get:

$$\tau_{rr}=\left(\frac{2\mu}{n\nu}\right)A_2r^{\nu-1}+\frac{c\xi\Theta_0\ln(r/r_0)}{\ln(r_i/r_0)}-\frac{c\xi\Theta_0}{\ln(r_i/r_0)}-\frac{\rho_0\omega^2r_0^mr^{2-m}}{(3-m)}+\frac{A_3}{r}, \quad (18)$$

where: A_3 is a constant of integration which can be determined.

Displacement components: displacement components are obtained by using Eq.(17) and Eq.(18) into second equation of Eq.(10) and using Eq.(3), we get

$$u=r-r\sqrt{1-\frac{2\nu}{E}\left[\frac{\rho_0\omega^2r_0^mr^{2-m}}{(3-m)}-\frac{A_3}{r}+\frac{\alpha E(2-c)\Theta_0}{\ln(r_i/r_0)}+\frac{2\alpha E(2-c)\Theta_0\ln(r/r_0)}{(1-c)\ln(r_i/r_0)}\right]}\,. \quad (19)$$

Applying boundary conditions Eq.(2) and Eq.(9) into Eq.(18) and Eq.(19), we get:

$$A_2=\frac{n\nu}{2\mu r_0^\nu}\left[l_0r_0+\frac{\rho_0\omega^2r_0^m(r_0^{3-m}-r_i^{3-m})}{(3-m)}+\frac{\alpha E(2-c)\Theta_0}{\ln(r_i/r_0)}(r_0-r_i)-\frac{2r_i\alpha E(2-c)\Theta_0}{(1-c)}\right],$$

$$A_3=\frac{\rho_0\omega^2r_0^mr_i^{3-m}}{(3-m)}+\frac{\alpha Ea(2-c)\Theta_0}{\ln(r_i/r_0)}+\frac{2r_i\alpha E\Theta_0(2-c)}{(1-c)}\,.$$

Substituting values of constants A_2 and A_3 into Eqs.(17), (18), and (19), respectively, we get transition stresses and displacement:

$$\tau_{\theta\theta}=\nu\left[l_0\left(\frac{r}{r_0}\right)^{\nu-1}+\left(\frac{r}{r_0}\right)^\nu\frac{\rho_0\omega^2r_0^m(r_0^{3-m}-r_i^{3-m})}{r(3-m)}+\alpha E(2-c)\Theta_0\left\{\left(\frac{1}{\nu}\right)\frac{\ln(r/r_0)}{\ln(r_i/r_0)}-\frac{2r_i}{r(1-c)}\left(\frac{r}{r_0}\right)^\nu+\frac{(r_0-r_i)}{r\ln(r_i/r_0)}\left(\frac{r}{r_0}\right)^\nu\right\}\right], \quad (20)$$

$$\tau_{rr}=l_0\left(\frac{r}{r_0}\right)^{\nu-1}+\frac{\rho_0\omega^2r_0^m}{r(3-m)}\left[(r_0^{3-m}-r_i^{3-m})\left(\frac{r}{r_0}\right)^\nu-r^{3-m}+r_i^{3-m}\right]+\frac{\alpha E(2-c)\Theta_0}{\ln(r_i/r_0)}\left[\left(\frac{r_0-r_i}{r}\right)\left(\frac{r}{r_0}\right)^\nu+\ln(r/r_0)-1+\frac{r_i}{r}\right]+$$

$$+\frac{2\alpha E(2-c)\Theta_0}{(1-c)}\left[\frac{r_i}{r}\left(1-\left(\frac{r}{r_0}\right)^\nu\right)\right], \quad (21)$$

$$u=r-r\sqrt{1-\frac{2\nu}{E}\left[\frac{\rho_0\omega^2r_0^m}{r(3-m)}[r^{3-m}-r_i^{3-m}]+\frac{\alpha E(2-c)\Theta_0(r-r_i)}{r\ln(r_i/r_0)}+\frac{2\alpha E(2-c)\Theta_0}{(1-c)}\left[\frac{\ln(r/r_0)}{\ln(r_i/r_0)}-\frac{r_i}{r}\right]\right]}\,, \quad (22)$$

and

$$\tau_{rr}-\tau_{\theta\theta}=l_0\left(\frac{r}{r_0}\right)^{\nu-1}(1-\nu)+\frac{\rho_0\omega^2r_0^m}{r(3-m)}\left[(r_0^{3-m}-r_i^{3-m})\left(\frac{r}{r_0}\right)^\nu(1-\nu)-r^{3-m}+r_i^{3-m}\right]+\alpha E(2-c)\Theta_0\times$$

$$\times\left[\left(\frac{r_0-r_i}{r\ln(r_i/r_0)}\right)\left(\frac{r}{r_0}\right)^\nu(1-\nu)+\frac{2r_i}{r(1-c)}+\frac{1}{\ln(r_i/r_0)}\left(\frac{r_i}{r}-1\right)+\frac{2r_i}{r(1-c)}\left(\frac{r}{r_0}\right)^\nu(\nu-1)\right]. \quad (23)$$

Non-dimensional components: $R_0 = r_i/r_0$, $\sigma_r = \tau_{rr}/Y$, $\sigma_\theta = \tau_{\theta\theta}/Y$, $U = u/r_0$, $\Theta_1 = \alpha E\Theta_0/Y$, $\Omega^2 = \rho_0\omega^2 r_0^2/Y$, $H = Y/E$, and $L_0 = l_0/Y$.

Maximum values of stresses: from Eq.(23), it has been seen that the value of transition stress ($\tau_{rr} - \tau_{\theta\theta}$) is maximum at the internal surface and yielding will occur at $r = r_i$ of the rotating disc.

Initial yielding stage: the maximal value $|\tau_{rr} - \tau_{\theta\theta}|$ arises at $r = r_i$ which depends upon the values of m and c, respectively. For yielding at $r = r_i$, Eq.(23) becomes:

$$\left|\tau_{rr}-\tau_{\theta\theta}\right|_{r=r_i} = l_0(1-\nu)\left(\frac{r_i}{r_0}\right)^{\nu-1} + \frac{\rho_0\omega^2 r_0^m}{r_i(3-m)}(1-\nu)(r_0^{3-m}-r_i^{3-m})\left(\frac{r_i}{r_0}\right)^{\nu} + \alpha E(2-c)\theta_0 \times$$

$$\times\left\{\frac{r_0-r_i}{r_i\ln(r_i/r_0)}\left(\frac{r_i}{r_0}\right)^{\nu}(1-\nu)+\frac{2}{(1-c)}+\frac{2}{(1-c)}\left(\frac{r_i}{r_0}\right)^{\nu}(\nu-1)\right\}\equiv Y\,.$$

Angular speed for initial yielding stage:

$$\Omega_i^2 = \frac{\rho_o\omega_i^2 r_0^2}{Y} = \frac{(3-m)}{\left(1-R_0^{3-m}\right)\left(\frac{r_i}{r_0}\right)^{\nu-1}(1-\nu)}\left[1-\left(\frac{L_0}{Y}\right)\left(\frac{r_i}{r_0}\right)^{\nu-1}(1-\nu)-\frac{\alpha E\Theta_0}{Y}\left[\frac{(1-r_i/r_0)}{\ln R_0}\left(\frac{r_i}{r_0}\right)^{\nu-1}+\frac{2}{\nu}-\frac{2}{(1-c)}\left(\frac{r_i}{r_0}\right)^{\nu}\right]\right]\equiv Y\,. \quad (24)$$

Stress distribution, angular speed and displacement: Eqs.(20), (21), (24) and (22), in non-dimensional form become:

$$\sigma_\theta = \nu\left[L_0R^{\nu-1}+\frac{\Omega_i^2R^{\nu-1}(1-R_0^{3-m})}{(3-m)}\right]+\Theta_1(2-c)\left[\frac{\ln R}{\ln R_0}-\frac{2R_0}{(2-c)}R^{\nu-1}+\frac{(1-R_0)\nu}{\ln R_0}R^{\nu-1}\right], \quad (25)$$

$$\sigma_r = L_0R^{\nu-1}+\frac{\Omega_i^2}{R(3-m)}\left[(1-R_0^{3-m})R^{\nu}-R^{3-m}+R_0^{3-m}\right]+\frac{\Theta_1(2-c)}{\ln R_0}\left[(1-R_0)R^{\nu-1}+\ln R-1+\frac{R_0}{R}\right]+\frac{2\Theta_1}{\nu}\left[\left(\frac{R_0}{R}\right)(1-R^{\nu})\right], \quad (26)$$

$$\Omega_i^2 = \frac{\rho_o\omega_i^2r_0^2}{Y} = \frac{(3-m)}{(1-R_0^{3-m})R_0^{\nu-1}(1-\nu)}\left[1-L_0R_0^{\nu-1}(1-\nu)-\Theta_1\left\{\frac{(1-R_0)}{\ln R_0}R_0^{\nu-1}+\frac{2}{\nu}-\frac{2}{(1-c)}R_0^{\nu}\right\}\right]\equiv Y\,, \quad (27)$$

And

$$U_i = R-R\sqrt{1-2\nu H\left[\frac{\Omega_i^2}{R(3-m)}\left[R^{3-m}-R_0^{3-m}\right]+\frac{(2-c)\Theta_1(R-R_0)}{R\ln R_0}+\frac{2\Theta_1}{\nu}\left[\frac{\ln R}{\ln R_0}-\frac{R_0}{R}\right]\right]}\,. \quad (28)$$

Fully plastic stage: Eq.(23) becomes fully-plastic (i.e. $c \to 0$ or $\nu = 1/2$) at the external surface of the disc:

$$\left|T_{rr}-T_{\theta\theta}\right|_{R=R_0} = \left[\frac{L_0}{2}+\frac{\rho_0\omega_f^2r_0^2}{(3-m)}\left[\frac{(1-R_0^{3-m})}{2}+R_0^{3-m}-1\right]+\alpha E\Theta_0\left[\frac{(1-R_0)}{\ln R_0}+2R_0+\frac{2(1-R_0)}{\ln R_0}\right]\right]\equiv Y^*\,.$$

Angular speed for fully-plastic stage:

$$\Omega_{f^*}^2 = \frac{\rho_o\omega_f^2r_0^2}{Y^*} = \left|\frac{2(3-m)}{(1-R_0^{3-m})}\right|\left[\left|1-\frac{L_0}{2}\right|+\Theta_1\left\{\frac{(1-R_0)}{\ln R_0}+2R_0+\frac{2(1-R_0)}{\ln R_0}\right\}\right], \quad (29)$$

where: $\omega_{f^*} = \dfrac{\Omega_{f^*}}{r_0}\sqrt{\dfrac{Y}{\rho_0}}$; and $\dfrac{\alpha E\Theta_0}{Y^*} = \Theta_1$.

Transition stress distribution and displacement: Eq. (25), Eq. (26) and Eq. (28) in non-dimensional form become:

$$\sigma_\theta^* = \frac{1}{2}\left[\frac{L_0}{\sqrt{R}}+\frac{\Omega_{f^*}^2(1-R_0^{3-m})}{\sqrt{R}(3-m)}\right]+2\Theta_1\left[\frac{\ln R}{\ln R_0}-\frac{R_0}{\sqrt{R}}+\frac{(1-R_0)}{2\sqrt{R}\ln R_0}\right], \quad (30)$$

$$\sigma_r^* = \frac{L_0}{\sqrt{R}}+\frac{\Omega_{f^*}^2}{R(3-m)}\left[\sqrt{R}(1-R_0^{3-m})-R^{3-m}+R_0^{3-m}\right]+\frac{2\Theta_1}{\ln R_0}\left[\frac{(1-R_0)}{\sqrt{R}}+\ln R-1+\frac{R_0}{R}\right]+4\Theta_1\left[\left(\frac{R_0}{R}\right)(1-\sqrt{R})\right], \quad (31)$$

and

$$U_f = R-R\sqrt{1-H\left[\frac{\Omega_{f^*}^2}{R(3-m)}\left[R^{3-m}-R_0^{3-m}\right]+\frac{2\Theta_1(R-R_0)}{R\ln R_0}+4\Theta_1\left[\frac{\ln R}{\ln R_0}-\frac{R_0}{R}\right]\right]}\,. \quad (32)$$

NUMERICAL RESULTS AND DISCUSSIONS

For calculating stress distribution, angular speed and displacement for initial/fully plastic stage of the disc made of rubber material (say $c = 0$ or $\nu = 0.5$) and copper material (say $c = 0.5$ or $\nu = 0.333$) based on the following numerical values: $r_i = 1$; $r_0 = 2$; $m = -2, 0, 2$; $H = 1, 1/2$ (constant

values); $L_0 = 50, 75$; $\alpha = 5.0 \times 10^{-5}$ degF^{-1} for $C_5H_8O_2$; $\Theta_0 = 0$ °F, 10000 °F, 15000 °F; $\Theta_1 = \alpha\Theta_0 = 0, 0.5, 0.75$. Table 1 shows the percentage (%) increase in angular speed required for initial yielding to the fully-plastic stage discussed numerically. It has been concluded that the copper disc requires higher percentage values (i.e. 59.36 %, 59.37 %, 59.38 %), whereas rubber disc (i.e. 42.64 %, 42.65 %, 42.66 %) at $\Theta_1 = 0$ to become fully plastic respectively. With increasing values of mechanical load and temperature, the percentage ratio of angular speed to become fully-plastic decreases.

In Figs. 2 and 3, curves are drawn between angular speed required for the initial/fully-plastic stage versus $R = r_i/r_0$ at Poisson's ratio $\nu = 0.5, 0.333$; loads $L_0 = 50, 75$ and density parameters $m = -2, 0, 2$, in respect. It has been seen from Fig. 2, that the rubber disc requires higher angular speed to yield at $r = r_i$ (i.e. an internal surface) as compared to the copper disc.

With increasing thermo-mechanical loading and density parameters, the values of angular speed are increased at the internal surface of the disc made of rubber material and also of copper material. It has been observed from Fig. 3, that the value of angular speed for fully-plastic state increases at the internal surface with increasing thermo-mechanical load and density parameters.

Curves are drawn between stress distribution and radii ratio $R = r/r_0$ (see Fig. 4) at the transition stage. From Fig. 4 we compute that the copper disc requires maximal radial stress at the internal surface in comparison to disc of rubber material. Further, by introduction of thermal condition, density parameters and loads, the values of radial/circumferential stress increase at the internal surface of the rotating disc.

Curves are plotted between displacement component and radii ratio $R = r/r_0$ at the transition/fully-plastic stage (see Fig. 5). It is observed that the value of the displacement component increases on the external surface of the copper/rubber disc for fully plastic stage. With the introduction of thermo-mechanical loading, the displacement component increases at the external surface of the disc, but the reverse results are obtained in case of density parameters, in respect.

CONCLUSIONS

The rubber disc requires higher angular speed to yield at the internal surface as compared to the disc made of copper material. With the effect of mechanical loading, the copper material disc is on the safer side of the design as compared to disc with temperature, because radial stress is less for the rotating disc without temperature as compared to the state with temperature, which leads to the idea of stress saving and minimizing the possibility of fracture of the rotating disc. With the effect of thermo-mechanical loading, the displacement component increases at the external surface of the disc, but reverse results are obtained in case of density parameters.

Abbreviations

λ, μ	Lame's constants
e_{kk}	first strain invariant
E	Young's modulus
c	compressibility factor
r_i, r_0	internal and external radius
ω	angular velocity
u, v, w	displacement components
ρ	density
α	coefficient of thermal expansion
ρ_0	density at outer surface
ν	Poisson's ratio
m	density parameter
τ_{ij}, ε_{ij}	stress and strain components
Y	yield stress
δ_{ij}	Kronecker's delta
d	constant
l_0	load applied at the outer surface
Θ	temperature
A, A_1, A_2, A_3	constants of integration
$R = r/r_0$, $R_0 = r_i/r_0$	radii ratio
σ_r	radial stress component (τ_{rr}/Y)
σ_θ	circumferential stress component ($\tau_{\theta\theta}/Y$)
Ω_i^2	angular speed for initial stage
Ω_f^2	angular speed for fully plastic stage

Table 1. Values of angular speed for initial yielding Ω_i^2 and fully plastic stage Ω_f^2 and $\nu = 0.5$ and 0.33.

Density param.	Angular speed	rubber (i.e. $\nu = 0.5$)					
		$\Theta_1 = 0$		$\Theta_1 = 0.5$		$\Theta_1 = 0.75$	
		Yielding starts at the bore ($r = r_i$)					
		$L_o = 50$	$L_o = 75$	$L_o = 50$	$L_o = 75$	$L_o = 50$	$L_o = 75$
$m = -2$	Ω_i^2	121.73	186.25	132.61	197.12	138.05	202.56
	Ω_f^2	247.74	376.77	252.19	381.22	254.41	383.44
$m = 0$	Ω_i^2	80.87	123.73	88.09	130.95	91.71	134.56
	Ω_f^2	164.57	250.29	167.53	253.24	168.99	254.72
$m = 2$	Ω_i^2	47.17	72.18	51.39	76.39	53.49	78.49
	Ω_f^2	96	146	97.73	147.73	98.58	148.58
$m = -2$	P %	42.64	42.21	37.88	39.04	35.75	37.58
$m = 0$	P %	42.65	42.22	37.89	39.05	35.76	37.59
$m = 2$	P %	42.66	42.23	37.90	39.06	35.77	37.60

Density param.	Angular speed	copper (i.e. $\nu = 0.333$)					
		$\Theta_1 = 0$		$\Theta_1 = 0.5$		$\Theta_1 = 0.75$	
		Yielding starts at the bore ($r = r_i$)					
		$L_0 = 50$	$L_0 = 75$	$L_0 = 50$	$L_0 = 75$	$L_0 = 50$	$L_0 = 75$
$m = -2$	Ω_i^2	97.54	148.74	109.38	160.58	115.29	166.51

	Ω_f^2	247.74	376.78	252.18	381.22	254.41	383.44
$m = 0$	Ω_i^2	64.79	98.81	72.66	106.68	76.59	110.61
	Ω_f^2	164.57	250.29	167.53	253.24	168.97	254.72
$m = 2$	Ω_i^2	37.79	57.64	42.39	62.23	44.68	64.52
	Ω_f^2	96	146.1	97.73	147.73	98.59	148.59
$m = -2$	P %	59.36	59.15	51.84	54.07	48.55	51.74
$m = 0$	P %	59.37	59.16	51.85	54.08	48.56	51.75
$m = 2$	P %	59.38	59.17	51.86	54.09	48.57	51.76

where: $P = (\sqrt{\Omega_f^2 / \Omega_i^2}\ -1)*100$ is the percentage (%) increase in angular speed; and $m = -2, 0, 2$; $\Theta_1 = 0, 0.5, 0.75$ and $\nu = 0.5, 0.33$.

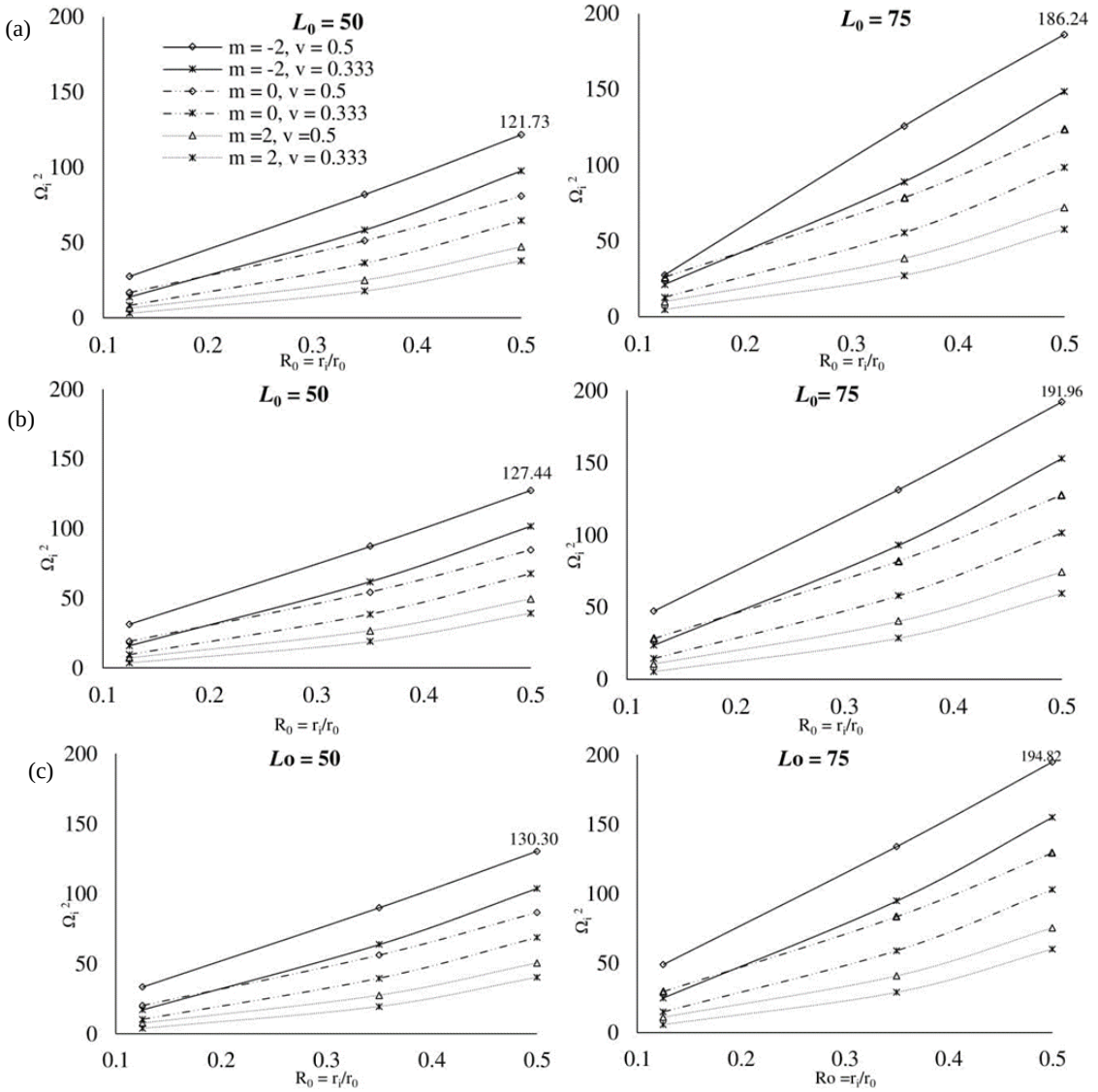

Figure 2. Angular speed vs. $R_0 = r_i / r_0$ for initial stage at: a) $\Theta_1 = 0$; b) $\Theta_1 = 0.50$; c) $\Theta_1 = 0.75$.

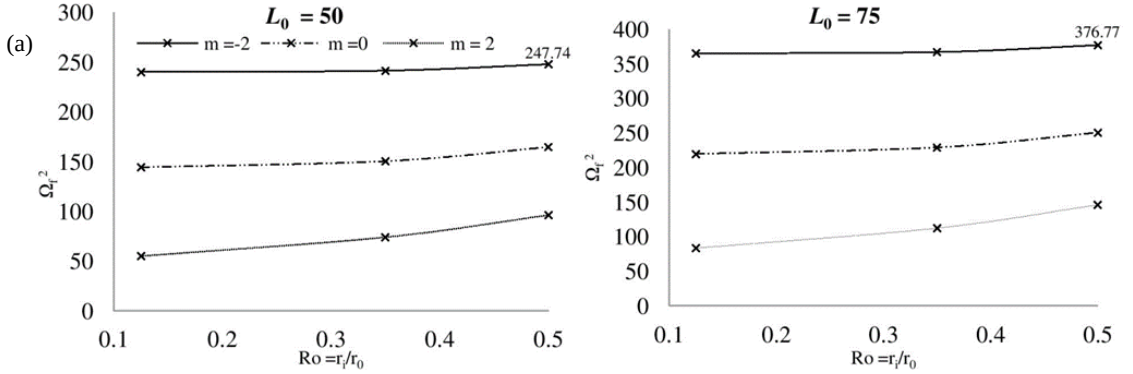

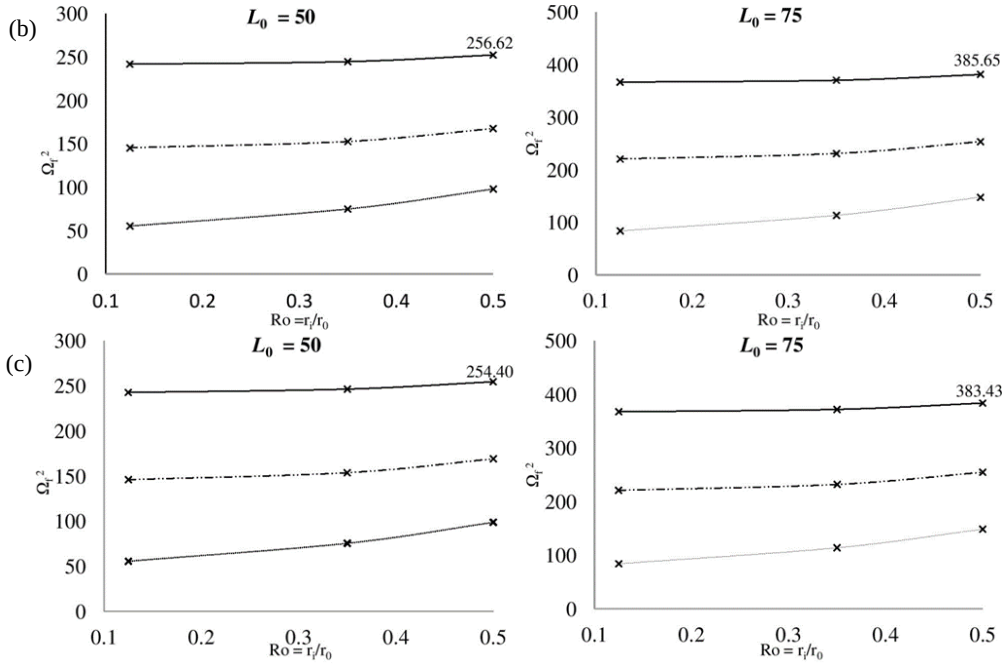

Figure 3. Angular speed vs. $R_0 = r_i / r_0$ for fully plastic stage at: a) $\Theta_1 = 0$; b) $\Theta_1 = 0.50$; c) $\Theta_1 = 0.75$.

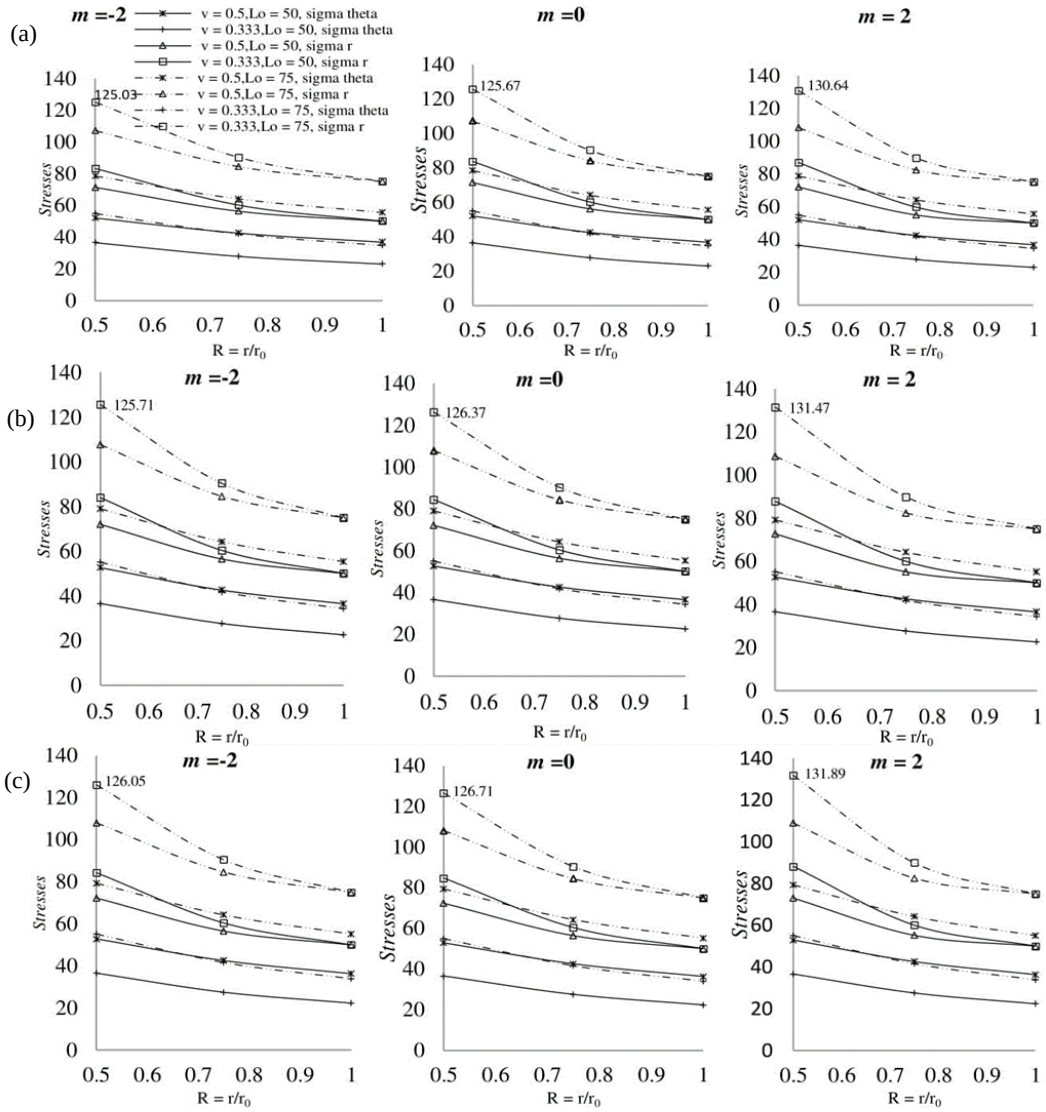

Figure 4. Stress distribution vs. $R = r / r_0$ at: a) $\Theta_1 = 0$; b) $\Theta_1 = 0.50$; c) $\Theta_1 = 0.75$.

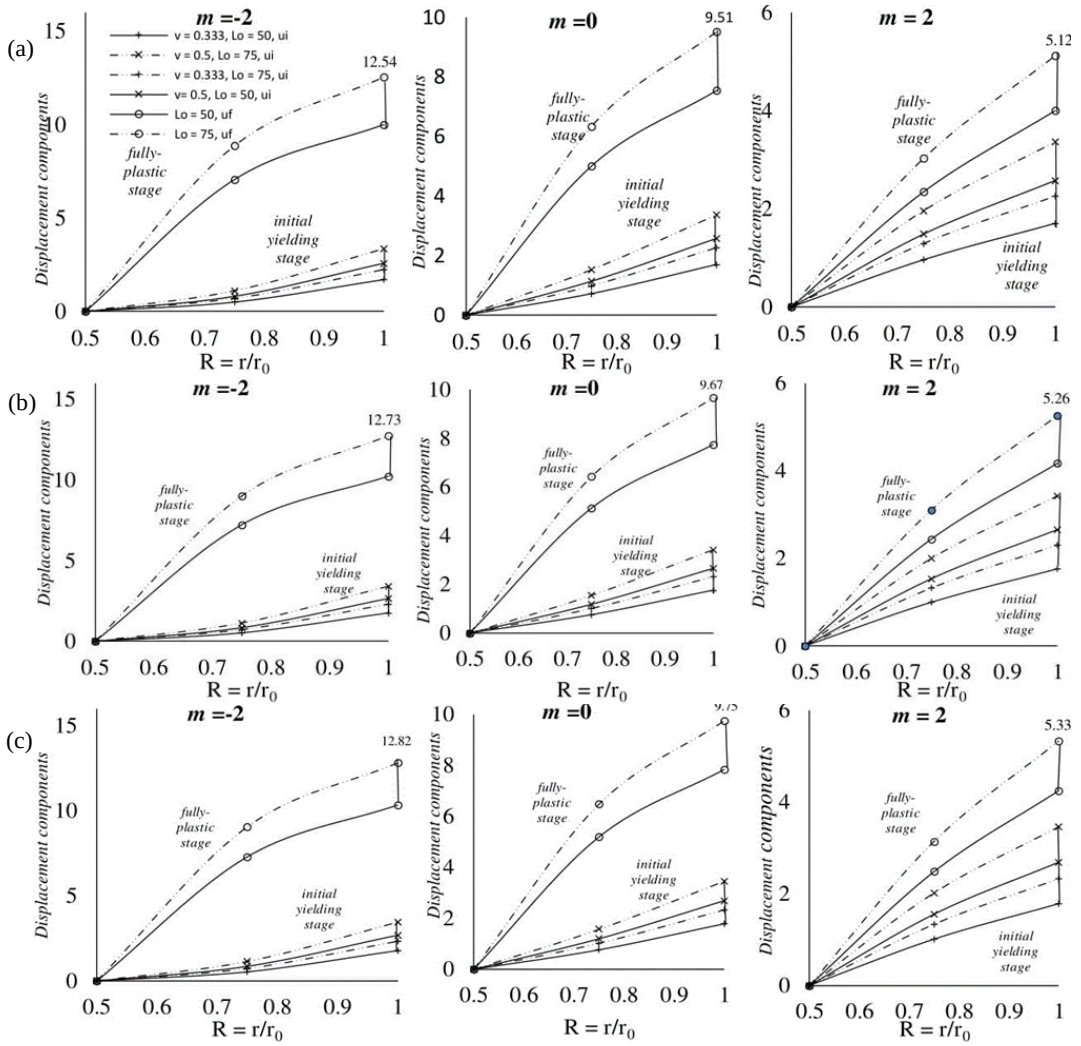

Figure 5. Displacement components vs. $R = r/r_0$ at: a) $\Theta_1 = 0$; b) $\Theta_1 = 0.50$; c) $\Theta_1 = 0.75$.

REFERENCES

1. Sokolnikoff, I.S., Mathematical Theory of Elasticity, 2nd Ed., McGraw-Hill Inc., New York, 1953.
2. Seth, B.R. (1962), *Transition theory of elastic-plastic deformation, creep and relaxation*, Nature, 195: 896-897. doi:10.1038/195896a0.
3. Parkus, H., Thermoelasticity, Springer-Verlag, Wien, 1976. doi: 10.1007/978-3-7091-8447-9
4. Güven, U., Atlay, O. (2000), *Elastic-plastic solid disk with nonuniform heat source subjected to external pressure*, Int. J Mech. Sci. 42(5): 831-842. doi: 10.1016/S0020-7403(99)00032-6
5. Eraslan, A.N., Akis, T. (2003), *On the elastic-plastic deformation of a rotating disk subjected to a radial temperature gradient*, Mech. Based Des. Struct. Machines, 31(4): 529–561. doi: 10.1081/SME-120023170
6. Alexandrova, N., Alexandrov, S. (2004), *Elastic-plastic stress distribution in a plastically anisotropic rotating disk*, J Appl. Mech. 71(3): 427-429. doi: 10.1115/1.1751183
7. Sayer, M., Topcu, M., Bektaş, N.B., Tarakcilar, A.R. (2005), *Thermo-elastic stress analysis in a thermoplastic composite disc*, Sci. Eng. Compos. Mater. 12(4): 251-260.
8. Faruk, S., Sayer, M. (2006), *Elasto-plastic thermal stress analysis in a thermoplastic composite disc under uniform temperature using FEM*, Math. Comp. Appl. 11(1): 31-39. doi: 10.3390/mca11010031
9. Altan, G., Topçu, M., Bektaş N.B., Altan, B.D. (2008), *Elastic-plastic thermal stress analysis of an aluminum composite disc under parabolic thermal load distribution*, J Mech. Sci. Technol. 22(12): 2318-2327. doi: 10.1007/s12206-008-0720-2
10. Bhowmick, S., Misra, D., Saha, K.N. (2008), *Approximate solution of limit angular speed for externally loaded rotating solid disk*, Int. J Mech. Sci. 50(2): 163-174. doi: 10.1016/j.ijmecsci.2007.07.004
11. Sen, F., Aldas, K. (2009), *Elastic-plastic thermal stress analysis in a thermoplastic composite disc applied linear temperature loads via FEM*, Adv. Eng. Software, 40(9): 813-819. doi: 10.1016/j.advengsoft.2009.01.012
12. Bayat, M., Saleem, M., Sahari, B.B. (2009), *Mechanical and thermal stresses in a functionally graded rotating disk with variable thickness due to radially symmetry loads*, Int. J Pres. Ves. Piping, 86(6): 357-372. doi: 10.1016/j.ijpvp.2008.12.006
13. Bhowmick, S., Misra, D., Saha, K.N. (2010), *Parametric study of externally loaded rotating discs under shrink fit*, Proc. Inst. Mech. Eng., Part C: J Mech. Eng. Sci. 224(11): 2525-2538. doi: 10.1243/09544062JMES1996
14. Damircheli, M., Azadi, M. (2011), *Temperature and thickness effects on thermal and mechanical stresses of rotating FG-disks*, J Mech. Sci. Technol. 25(3): 827-836. doi: 10.1007/s12206-011-0110-z
15. Kurşun, A., Topcu, M., Tetik, T. (2011), *Stress analysis of functionally graded disc under thermal and mechanical loads*, Procedia Eng. 10: 2949-2954. doi: 10.1016/j.proeng.2011.04.489

16. Hassani, A., Hojjati, M.H., Mahdavi, E. (2012), *Thermo-mechanical analysis of rotating disks with non-uniform thickness and material properties*, Int. J Pres. Ves. Piping, 98: 95-101. doi: 10.1016/j.ijpvp.2012.07.010
17. Kurşun, A., Topçu, M. (2013), *Thermal stress analysis of functionally graded disc with variable thickness due to linearly increasing temperature load*, Arab. J Sci. Eng. 38: 3531-3549. doi: 10.1007/s13369-013-0626-x
18. Thakur, P., Singh, S.B., Kaur, J. (2013), *Thickness variation parameter in a thin rotating disc by finite deformation*, FME Transactions, 41(2): 96-102.
19. Thakur, P., Singh, S.B., Kaur, J. (2014), *Elastic-plastic stresses in a thin rotating disk with shaft having density variation parameter under steady-state temperature*, Kragujevac J Sci. 36: 5-17.
20. Thakur, P., Singh, S.B., Lozanović Šajic, J. (2015), *Thermo elastic-plastic deformation in a solid disk with heat generation subjected to pressure*, Struct. Integ. and Life, 15(3): 135-142.
21. Kaur, J., Thakur, P., Singh, S.B. (2016), *Steady thermal stresses in a thin rotating disc of finitesimal deformation with mechanical load*, J Solid Mech. 8(1): 204-211.
22. Thakur, P., Verma, G., Pathania, D.S., Singh, S.B. (2017), *Elastic-plastic transition on rotating spherical shells in dependence of compressibility*, Kragujevac J Sci. 39(1): 5-16.
23. Thakur, P., Pathania, D., Verma, G., Singh, S.B. (2017), *Elastic-plastic stress analysis in a spherical shell under internal pressure and steady state temperature*, Struct. Integ. and Life, 17(1): 39-43.
24. Thakur, P., Sethi, M. (2018), *Creep damage modelling in a transversely isotropic rotating disc with load and density parameter*, Struct. Integ. and Life, 18(3): 207-214.
25. Thakur, P., et al. (2018), *Creep stresses and strain rates for a transversely isotropic disc having the variable thickness under internal pressure*, Struct. Integ. and Life, 18(1): 15-21.
26. Thakur, P., Sethi, M., Shahi, S., et al. (2018), *Exact solution of rotating disc with shaft problem in the elastoplastic state of stress having variable density and thickness*, Struct. Integ. and Life, 18(2): 128-134.
27. Thakur, P., Sethi, M., Shahi, S., et al. (2018), *Modelling of creep behaviour of a rotating disc in the presence of load and variable thickness by using Seth transition theory*, Struct. Integ. and Life, 18(2): 135- 142.
28. Sethi, M., Thakur, P., Singh, H.P. (2019), *Characterization of material in a rotating disc subjected to thermal gradient by using Seth transition theory*, Struct. Integ. and Life, 19(3): 151-156.
29. Thakur, P., et al. (2019), *Elastic-plastic stress concentrations in orthotropic composite spherical shells subjected to internal pressure*, Struct. Integ. and Life, 19(2): 73-77.
30. Thakur, P., Sethi, M. (2019), *Lebesgue measure in an elasto-plastic shell*, Struct. Integ. and Life, 19(2): 115-120.
31. Thawait, A.K., Sondhi, L., Sanyal, S., Bhowmick, S. (2019), *Stress and deformation analysis of clamped functionally graded rotating disks with variable thickness*, Mech. Mech. Eng. 23 (1): 202-221. doi: 10.2478/mme-2019-0027
32. Sethi, M. Thakur P. (2020), *Elastoplastic deformation in an isotropic material disk with shaft subjected to load and variable density*, J Rubber Res. 23: 69-78. doi: 10.1007/s42464-020-00038-8
33. Abdalla, H.M.A., Casagrande, D., Moro, L. (2020), *Thermo-mechanical analysis and optimization of functionally graded rotating disks*, The J Strain Anal. Eng. Des. 55(5-6): 159-171. doi: 10.1177/0309324720904793
34. Thakur, P., Gupta, N., Sethi, M., Gupta, K. (2020), *Effect of density parameter in a disk made of orthotropic material and rubber*, J Rubber Res. 23(3): 193-201. doi: 10.1007/s42464-020-00049-5
35. Thakur, P., Gupta, N., Gupta, K., Sethi, M. (2020), *Elastic-plastic transition in an orthotropic material disk*, Struct. Integ. and Life, 20(2): 169-172.
36. Thakur, P., Sethi M. (2020), *Elastoplastic deformation in an orthotropic spherical shell subjected to temperature gradient*, Math. Mech. Solids, 25(1): 26-34. doi: 10.1177/1081286519857128
37. Thakur, P., Sethi, M. (2020), *Creep deformation and stress analysis in a transversely material disc subjected to rigid shaft*, Mat. Mech. Solids, 25(1): 17-25. doi: 10.1177/1081286519857109.
38. Thakur, P., Kumar N., Sukhvinder (2020), *Elasto-plastic density variation in a deformable disk*, Struct. Integ. and Life, 20(1): 27-32.
39. Temesgen, A.G., Singh, S.B., Thakur, P. (2020), *Modelling of elastoplastic deformation of transversely isotropic rotating disc of variable density with shaft under a radial temperature gradient*, Struct. Integ. and Life, 20(2): 113-121.
40. Thakur, P., Chand, S., Sukhvinder et al. (2020), *Density parameter in a transversely and isotropic disc material with rigid inclusion*, Struct. Integ. and Life, 20(2): 159-164.
41. Temesgen, A.G., Singh, S.B., Thakur, P. (2020), *Modeling of creep deformation of a transversely isotropic rotating disc with a shaft having variable density and subjected to a thermal gradient*, Therm. Sci. Eng. Progress, doi: 10.1016/j.tsep.2020.100745
42. Thakur, P., Kumar, N., Sethi, M. (2021), *Elastic-plastic stresses in a rotating disc of transversely isotropic material fitted with a shaft and subjected to thermal gradient*, Meccanica, 56: 1165-1175. doi: 10.1007/s11012-021-01318-2
43. Thakur, P., Sethi, M., Gupta, N., Gupta, K. (2021), *Thermal effects in rectangular plate made of rubber, copper and glass materials*, J Rubber Res. 24(1): 147-155. doi: 10.1007/s42464-020-00080-6
44. Temesgen, A.G., Singh, S.B., Thakur, P. (2021), *Elastoplastic analysis in functionally graded thick-walled rotating transversely isotropic cylinder under a radial temperature gradient and uniform pressure*, Math. Mech. Solids, 26(1): 5-17. doi: 10.1177/1081286520934041
45. Kumar, N., Thakur, P. (2021), *Thermal behaviour in a rotating disc made of transversely isotropic material with rigid shaft*, Struct. Integ. and Life, 21(3): 217-223.